

Principal Component Analysis for the Whole Facial Image With Pigmentation Separation and Application to the Prediction of Facial Images at Various Ages

Saori Toyota, Izumi Fujiwara, and Misa Hirose

Graduate School of Advanced Integration Science, Chiba University, Chiba, Japan

E-mail: either.will.do@gmail.com

Nobutoshi Ojima

Global R&D Beauty Creation, Kao Corporation, Tokyo, Japan

Keiko Ogawa-Ochiai

Clinic of Japanese-Oriental (Kampo) Medicine, Department of Otorhinolaryngology & Head and Neck Surgery, Kanazawa University Hospital Kanazawa, Japan

Norimichi Tsumura

Graduate School of Advanced Integration Science, Chiba University, Chiba, Japan

Abstract. In this article, principal component analysis is applied to pigmentation distribution in the whole face to obtain feature values, and the relationship between the obtained feature vectors and age is estimated by multiple regression analysis to simulate the changes of facial images in women of ages 10 to 80. Since the human face receives more attention than other body parts, a change of a small quantity of the features in a face makes a large difference to its appearance. We can divide the features into two categories. One category is physical features such as skin condition and shape, and the other is physiological features, which are influenced by age and health. In the beauty industry, the synthesis of skin texture is based on these two kinds of feature values. Previous works have analyzed only small areas of skin texture. By morphing the shapes of facial images to that of an average face and extending the analyzed area to the whole face, the authors' method can analyze pigmentation distributions in the whole face and simulate the appearance of a face as a function of changing the person's age. © 2014 Society for Imaging Science and Technology.
[DOI: 10.2352/J.ImagingSci.Technol.2014.58.2.020503]

INTRODUCTION

Human faces receive a lot of attention in comparison with other body parts. We can obtain a great deal of information from their appearance, such as individual features, race, age, emotion, gender, and health condition. A change of a small quantity of features makes a large difference to the appearance of a face.

Recently, applications that change the appearance of faces have been put into practical use and continue to be developed with the advance of technology in various fields. Women especially have a strong interest in the

appearance of their face or skin, and so applications that improve facial appearance are in high demand. However, conventional applications simply improve appearance, and these applications do not consider personal features.

In the beauty industry, applications that change the facial appearance by using facial images are also required to predict facial images under various conditions. Computer-suggested skin analyses are often applied. Computers measure skin information such as moisture level or analyze the roughness of skin texture. Additionally, computer-suggested simulations that change the facial appearance by using facial images are used to simulate makeup or predict the effect of basic skin care products. With these computer applications, users who wish to change their skin texture with makeup can obtain simulation results without trial-and-error or long-term use of a product. These applications are expected to synthesize the skin texture physically or simulate skin color based on two kinds of feature value. One kind is physical features, such as individual qualities and structures obtained from faces, and the other kind is physiological features, such as age and health condition. A cosmetic simulator is one example of the above applications that can change the facial appearance. The simulator applies digital makeup with skin information on moisture level, texture, etc. The simulator can advise customers when they are choosing cosmetics. This application can use numerous techniques, such as obtaining, analyzing and synthesizing skin texture or facial structure information, and estimating skin color changes.

The facial appearance has been reconstructed or simulated by previous methods in many studies. For example, three-dimensional facial data or two-dimensional facial images are used to reconstruct facial appearance,^{1,2} or the changes of facial appearance are simulated for makeup,^{3,4} for various ages,⁵ and for race.⁶ Typical examples of simulation

Received Aug. 28, 2013; accepted for publication July 9, 2014; published online Aug. 8, 2014. Associate Editor: Yeong-Ho Ha.

1062-3701/2014/58(2)/020503/11/\$25.00

methods are introduced in the following. Makino et al. developed a practical lighting reproduction technique to reproduce the appearance of a face under arbitrary lighting conditions.^{1,2} They reproduced the appearance of a face by combining image-based components, including captured live video images, as well as model-based components, including three-dimensional shapes, surface normals and the bidirectional reflectance distribution function (BRDF). Scherbaum et al. presented computer-suggested makeup.³ They obtained detailed feature values such as the three-dimensional structure, a normal map, subsurface scattering, specular and diffuse reflectance, and glossiness by using facial photographs taken with different light sources. Guo et al. also proposed a digital makeup system, in which makeup information was extracted from facial images with makeup already applied, and the extracted information was added to another facial image without makeup.⁴ Appropriate results for personal features could be obtained in all of these studies, because they used a person's own three-dimensional structure. In these studies, however, large systems are required to obtain information and it is difficult to put them into practical use. On the other hand, Lantis et al. proposed a framework that can be used for the simulation of aging effects on new face images to predict how an individual might look in the future or might have looked in the past.⁵ In their method, the facial structure is changed by applying principal component analysis (PCA) and a genetic algorithm to landmarks obtained from monochrome images. Chalothorn et al. extracted racial differences between Japanese and Thai people.⁶ They applied PCA to skin texture and structure for the classification of race. PCA is used extensively as a method to obtain feature values comparatively easily. In this article, PCA is applied for pigmentation distributions in whole facial images to obtain feature values.

In a general case, RGB values are used for the processing of facial images into skin texture information. However, RGB values are dependent on changes in the light source or characteristics of the camera, and they do not consider the skin structure and properties. Skin color mainly consists of melanin and hemoglobin pigmentations. Tsumura et al. proposed a method to extract melanin pigmentation and hemoglobin pigmentation from a single skin color image by independent component analysis.^{7,8} By using independent component analysis, melanin and hemoglobin colors can be obtained without the effects of changed light sources or the characteristics of a camera.

Okaguchi et al. obtained hierarchical pigmentation distributions from image pyramid analysis and set image histograms as feature values.⁹ Furthermore, they analyzed the principal components of skin unevenness by applying PCA to feature values in the histograms and simulated the skin texture, which has arbitrary physiological features based on multiple regression analysis between the physiological features and the feature values in the histograms. This research showed that skin texture having uneven pigmentation can be synthesized physically to achieve an appropriate

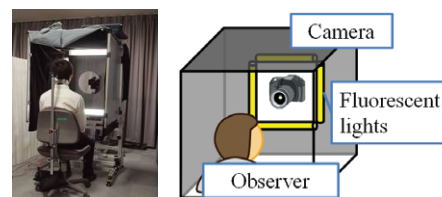


Figure 1. Overview of the imaging system.

skin appearance. However, processing by this method is restricted to small skin areas, not the whole face.

In this article, we apply PCA to whole facial images by extending the skin areas to analyze the pigmentation unevenness in the whole face. Additionally, we use multiple regression analysis to simulate the facial texture, which has arbitrary physiological features based on the relationship between the obtained principal components and feature vectors.

In the next section we describe our approach. First, we present the construction of a facial image database, and morph the facial images to an average face. Then we extract the melanin and hemoglobin pigmentations from a single skin color image by independent component analysis.⁷ Next, we describe the method to apply PCA to pigmentation distributions and the method to analyze the principal components of uneven pigmentation. Finally, we simulate the appearance of a face of arbitrary age after estimating the relationship between the obtained principal components and feature values by multiple regression analysis. In the third section, we discuss our results. In the fourth section, we present the conclusions of our research.

PROPOSED METHOD

This section shows the method to obtain feature values of pigmentation unevenness in the whole face and the method to simulate facial appearance with arbitrary physiological features. The overview of the process is as follows.

- Step 1. Construction of a facial image database.
- Step 2. Morphing of facial images to obtain an average face.
- Step 3. Extraction of melanin and hemoglobin pigmentations by independent component analysis.
- Step 4. Analysis of the principal components of uneven pigmentation by PCA.
- Step 5. Estimation of the appearance of a face by multiple regression analysis and synthesis of facial images.

In the following, we describe the details of the above processes.

Construction of a Facial Image Database

We took photographs of women who ranged in age from 10 to 80 and constructed a database. The number of subjects was 202. Figure 1 shows an overview of the imaging system. In the imaging system, ambient light sources were blocked by blackout curtains. The four fluorescent lights were set so that they surrounded the camera as the light source.

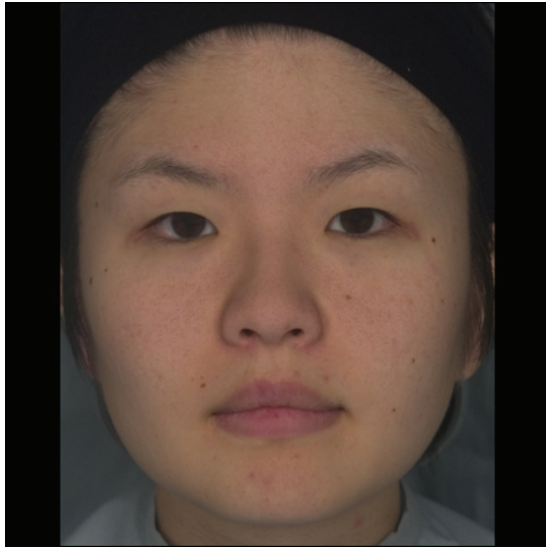


Figure 2. Sample of a captured facial image in the database.

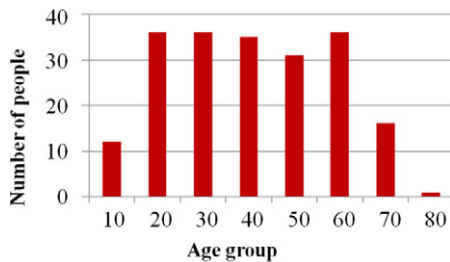


Figure 3. Distribution of ages in the database.

We took images using a digital camera (Nikon D3X) and used a chin support to prevent movement of the subject's face. We obtained facial images without specular reflectance by setting polarization filters in front of the camera and positioning the light sources to be perpendicular to each other. Figure 2 shows a sample of a captured facial image in the database. We obtained the ages of people in the database as physiological features in this article. The distribution of ages in the database is shown in Figure 3.

Morphing of Facial Images to an Average Face

We morphed the shapes of the facial images into that of an average face to remove the influence of individual facial shapes for a high degree of accuracy in the PCA. The facial image synthesis system FUTON (Foolproof UTilities for facial image manipulatiON system), which was developed by Mukaida et al.,¹⁰ was used to morph the facial images. FUTON helps in the extraction of significant facial features. Each facial image was morphed to an average face after creating an average facial image in the database. Figure 4(a) and (b) show an average face and a normalized image after morphing the image shown in Fig. 2. It can be recognized that the structures of the image are normalized and the skin texture information is saved. In addition, since the eyes and lips have different pigmentation properties in comparison with the pigmentation distribution of skin, we removed these areas to prevent any influence when we applied PCA. The eye and lip areas were removed from selected area by connecting landmarks of the average face. An example of an average image with the removed areas is shown in Fig. 4(c).

Extraction of Melanin and Hemoglobin Pigmentations

Human skin is constructed from two types of layers, the epidermis and the dermis. The epidermis layers mainly contain the melanin pigmentation, and the dermis layers mainly contain the hemoglobin pigmentation. Entering incident light passes the epidermis and dermis, and light is emitted from the surface of the skin. Assuming that the modified Lambert-Beer law is satisfied for the incident light in the skin layer,¹¹ we can state that the incident light is absorbed by the melanin and the hemoglobin pigmentations, and changes of skin color depend on the distributions of these two pigmentations. The modified Lambert-Beer law describes the influence of light scattering in biological tissue. In this case, the diffuse reflection is written as follows:

$$L(x, y, \lambda) = \exp \left\{ -\rho_m(x, y)\sigma_m(\lambda)l_m(\lambda) - \rho_h(x, y)\sigma_h(\lambda)l_h(\lambda) \right\} E(x, y, \lambda). \quad (1)$$

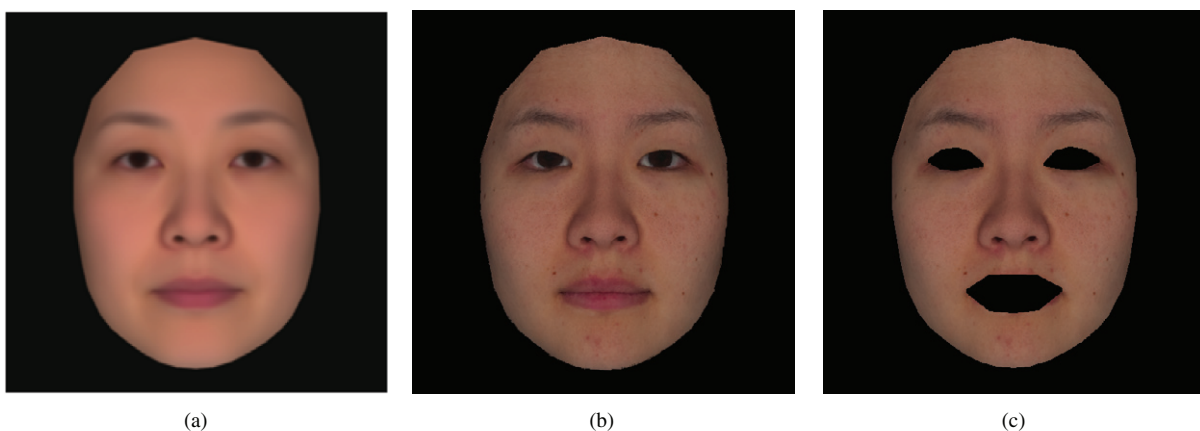


Figure 4. Image processed by Foolproof UTilities for facial image manipulatiON system (FUTON)¹⁰: (a) average face, (b) sample of normalized image by morphing, (c) sample of image where unneeded areas are removed.

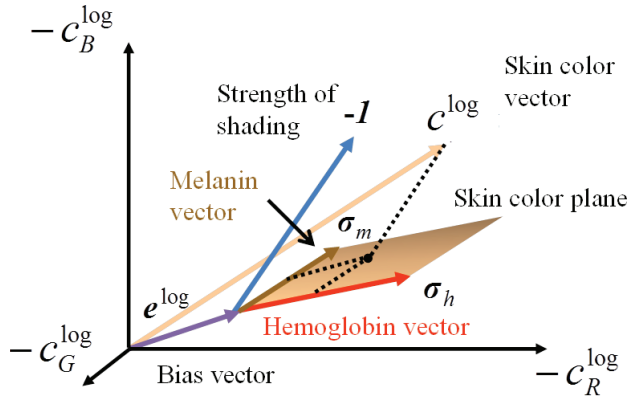


Figure 5. Overview of independent component analysis.

The modified Lambert–Beer law uses the mean pass length of photons in the medium as the depth of the medium. Here, λ is the wavelength, $E(x, y, \lambda)$ and $L(x, y, \lambda)$ are the incident spectral irradiance and reflected spectral radiance, respectively, at position (x, y) on the surface. The pigmentation densities and spectral absorption cross-sections of melanin and hemoglobin are $\rho_m(x, y)$, $\rho_h(x, y)$, $\sigma_m(x, y)$, $\sigma_h(x, y)$, respectively. Spectral absorption cross-sections are defined as cross-sections that correspond to the photon quantities absorbed from the incident light, because part of the incident light is absorbed into the pigmentation. Finally, $l_m(\lambda)$ and $l_h(\lambda)$ are the mean pass lengths of photons in the epidermis and dermis layers, respectively.

Surface reflection is removed by polarizers placed in front of both the camera and the light source. The sensor response c_i ($i = R, G, B$) from a digital camera is written as

$$\begin{aligned} c_i(x, y) &= k \int L(x, y, \lambda) s_i(\lambda) d\lambda \\ &= k \int \exp \left\{ -\rho_m(x, y) \sigma_m(\lambda) l_m(\lambda) \right. \\ &\quad \left. - \rho_h(x, y) \sigma_h(\lambda) l_h(\lambda) \right\} E(x, y, \lambda) s_i(\lambda) d\lambda, \quad (2) \end{aligned}$$

where $s_i(\lambda)$ ($i = R, G, B$) is the spectral sensitivity of the digital camera, and k is a constant value determined

from the gain of the camera. From the previous research by Drew et al.,¹² we treat the sensitivities as a delta function $s_i(\lambda) = \delta(\lambda - \lambda_i)$. Furthermore, we suppose that the lighting environment is distant and that its spectrum does not vary with direction. Then, the irradiance can be written as $E(x, y, \lambda) = p(x, y) \bar{E}(\lambda)$, where $p(x, y)$ is the shape-included shading variation. The irradiance variation is the parameter that encodes the difference of shading, which is influenced by facial shape in two-dimensional images. In our research, we define the shading variation as $(1, 1, 1)$ to assume that the shading is a vector of intensity 1. Therefore, Eq. (2) can be simplified as follows:

$$c_i(x, y) = k \exp \left\{ -\rho_m(x, y) \sigma_m(\lambda) l_m(\lambda) - \rho_h(x, y) \sigma_h(\lambda) l_h(\lambda) \right\} p(x, y) E(\lambda_i). \quad (3)$$

When we take the logarithm of Eq. (3), the following equations are obtained by vector and matrix formulation:

$$c^{\log}(x, y) = -\rho_m(x, y) \sigma_m - \rho_h(x, y) \sigma_h + p^{\log}(x, y) \mathbf{1} + e^{\log}, \quad (4)$$

where

$$\begin{aligned} c^{\log} &= [\log(c_R(x, y)), \log(c_G(x, y)), \log(c_B(x, y))]^t, \\ \sigma_m &= [\sigma_m(\lambda_R) l_m(\lambda_R), \sigma_m(\lambda_G) l_m(\lambda_G), \sigma_m(\lambda_B) l_m(\lambda_B)]^t, \\ \sigma_h &= [\sigma_h(\lambda_R) l_h(\lambda_R), \sigma_h(\lambda_G) l_h(\lambda_G), \sigma_h(\lambda_B) l_h(\lambda_B)]^t, \\ \mathbf{1} &= [1, 1, 1]^t, \\ e^{\log} &= [\log(E(\lambda_R)), \log(E(\lambda_G)), \log(E(\lambda_B))], \\ p^{\log}(x, y) &= \log(p(x, y)) + \log(k) \end{aligned}$$

are used to write Eq. (4) in simple terms. Then, the observed signal \mathbf{v}^{\log} is represented by the weighted linear combination of three vectors σ_m , σ_h , $\mathbf{1}$ with the bias vector e^{\log} . Figure 5 shows an overview of these processes in independent component analysis. The melanin and hemoglobin pigmentation density vectors can be obtained by applying independent component analysis to samples of the skin color datasets plotted in RGB density space. When a new skin color is given, its vector is projected onto the skin color plane by using shading variation. The melanin and

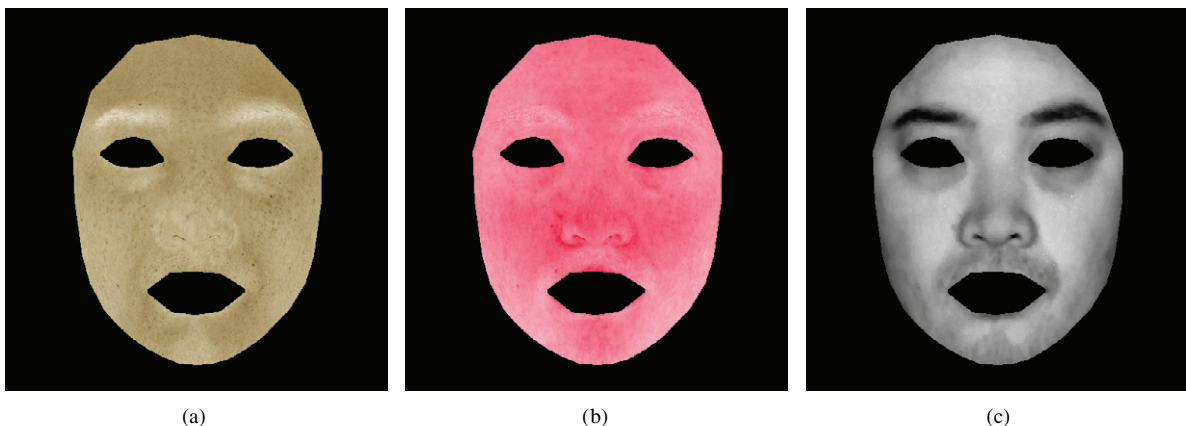


Figure 6. Results of independent component analysis of extracted pigmentation components: (a) melanin, (b) hemoglobin, (c) shading components.

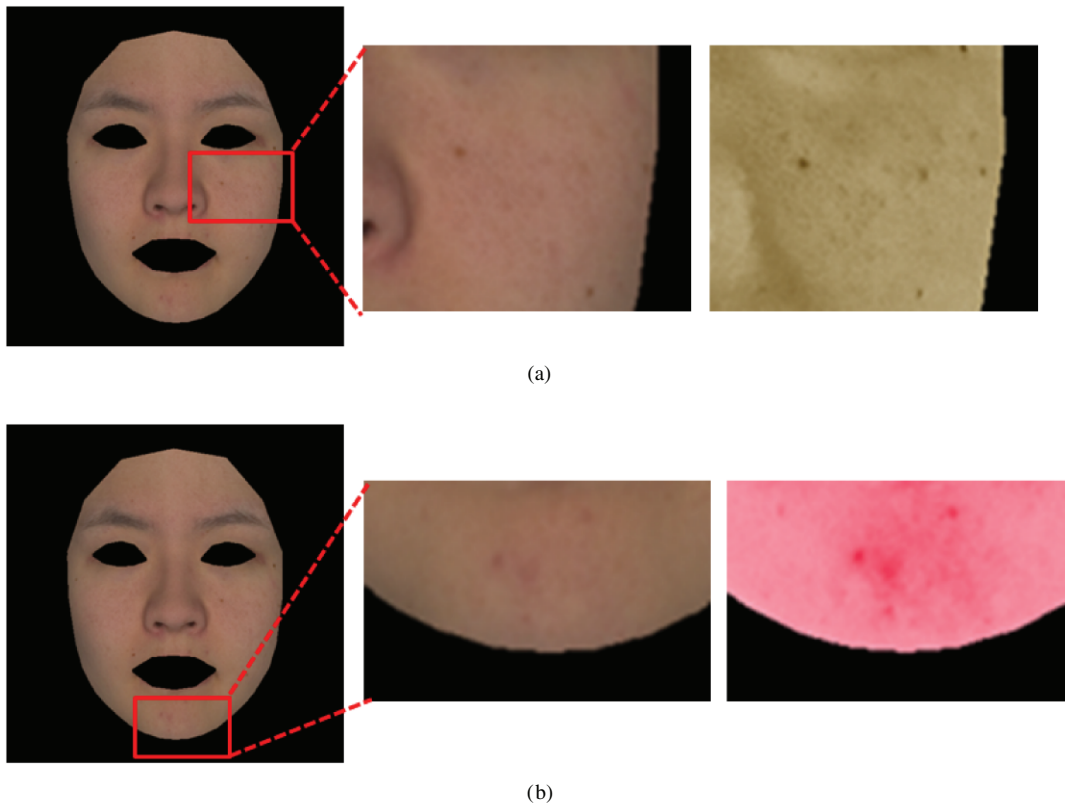


Figure 7. Close-up images of results of extracted pigmentation components: (a) cheek area of melanin component, (b) jaw area of hemoglobin component.

hemoglobin pigmentation densities are obtained when the projected skin color is reprojected onto each pigmentation density vector.

Figures 6(a) and (b) are the extracted melanin and hemoglobin pigmentations and (c) is the shading in the whole facial image. A close-up of the cheek area in Fig. 6(a) is shown in Figure 7(a), and a close-up of the jaw area in Fig. 6(b) is shown in Fig. 7(b). We can recognize the mole and pigmented spots from the close-up image of the cheek area of the melanin component shown in Fig. 7(a). Redness caused by pimples can be recognized from the close-up image of the jaw area of the hemoglobin component shown in Fig. 7(b). The shading component in Fig. 6(c) can be used to recognize the facial shape. In this article, the features of each component are processed separately.

Analysis of the Principal Components of Uneven Pigmentation

In this subsection, we describe the method to obtain feature values of uneven pigmentation in a whole face by applying PCA to the pigmentation distribution.¹³ PCA is a basic method of multivariate statistical analysis. PCA calculates the maximum variance vector for an arbitrary data group and defines the first principal component as a new index. Next, the second principal component is defined as perpendicular to the first principal component. This analysis continues in the next principal component. After PCA, the n -dimensional l th vector in dataset x_{ln} can be represented as

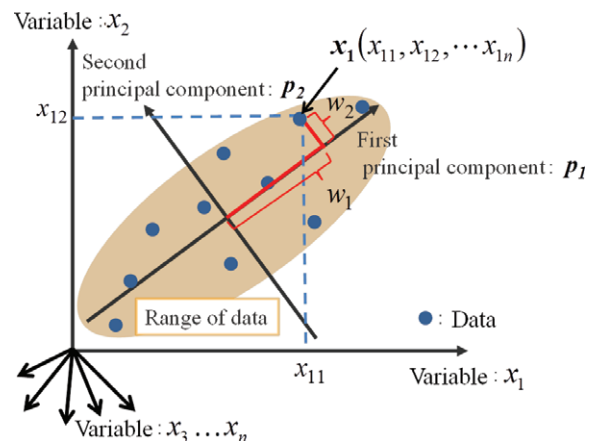


Figure 8. Overview of principal component analysis.

the approximated vector \hat{x}_l , which is defined by the principal component vector p_m and the weight value vector w_{lm} as follows:

$$\hat{x}_l(x_{l1}, x_{l2}, \dots, x_{ln}) = \sum_{m=1}^M w_{lm} p_m, \quad (5)$$

where M is the number of principal components used in the approximation, p_m is the m th principal component vector, and w_{lm} is the weight value for each m th principal component, as shown in Figure 8.



Figure 9. Results of PCA: (a) melanin components, (b) hemoglobin components, (c) shading components.

We applied PCA to a facial image composed of 512×512 pixels. One pixel is assigned as one element in the vector, and then one facial image is assigned as one point in a 262 144 (512×512) dimensional space. The total number of facial images used was 202, so we had 202 points in 262 144 dimensional spaces.

In the PCA, we obtained 201 principal components. Examples of principal component images applied to melanin components, hemoglobin components, and shading components are shown in Figure 9(a), (b), and (c), respectively. The numbers at the top left of the images represent the number of principal components sorted by the contribution

rate. We thus could obtain the principal components of the pigmentation distribution in the whole face.

Facial Color Image Synthesis

Using multiple regression analysis, we estimated the relationship between the obtained feature values of pigmentation unevenness and age as the physiological feature values. The principal components were resorted based on the order of higher correlation with age, and some principal components were selected so that their determination coefficient was calculated to be 0.7. After the weight of each principal component was modulated based on

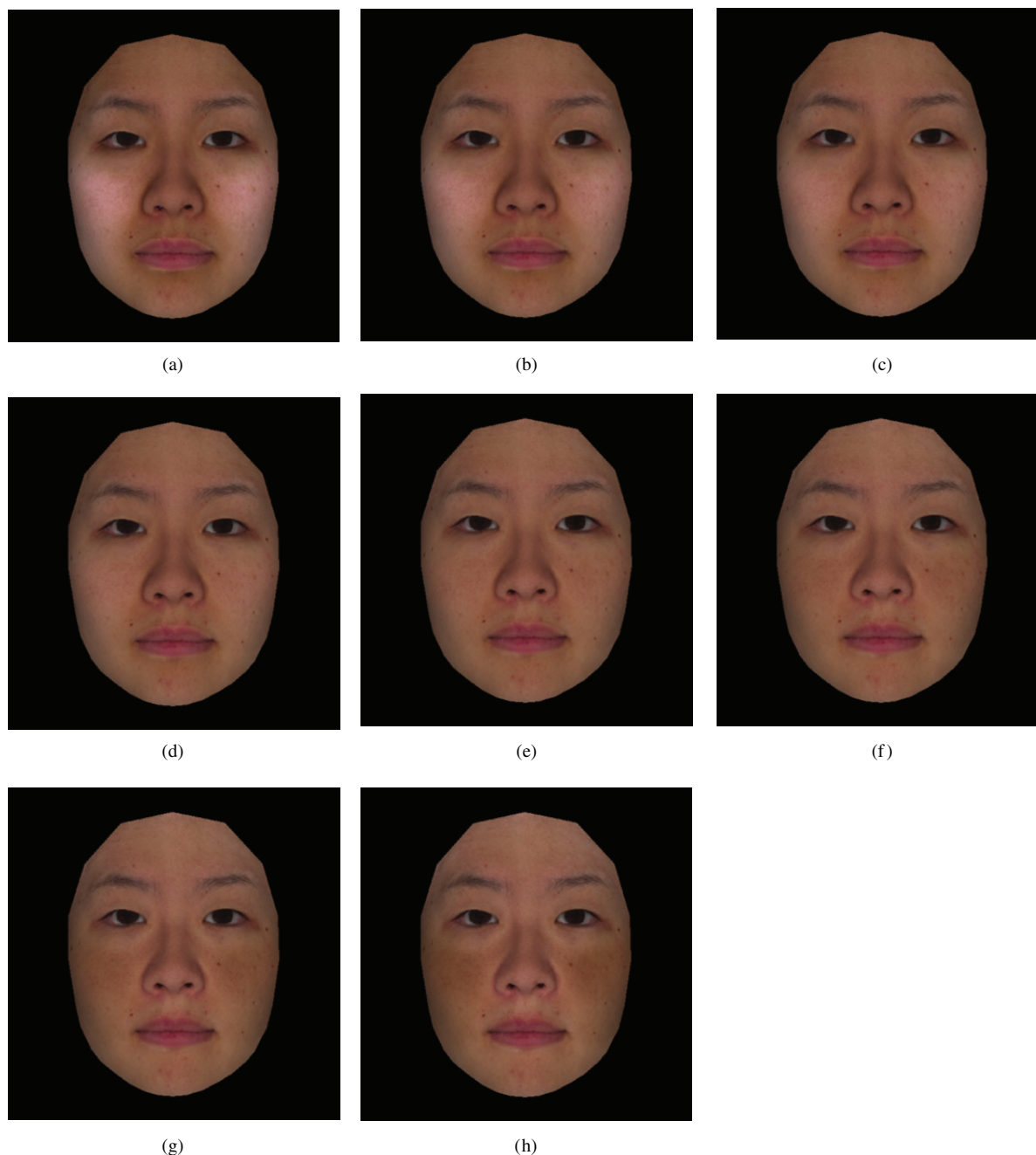


Figure 10. Results of facial appearance by age-related changes in melanin components: (a) 10s, (b) 20s, (c) 30s, (d) 40s, (e) 50s, (f) 60s, (g) 70s, (h) 80s.

the relationship between principal components and age, the melanin, hemoglobin, and shading components were simulated by age-related changes. Figures 10–13 show the age-related changes. Fig. 10(a)–(h) show the images where the melanin components are changed. Fig. 11(a)–(h) show the images where the hemoglobin components are changed. Fig. 12(a)–(h) show the images where the shading components are changed. When all these components were synthesized, the appearance of the face was simulated by age-related changes. Fig. 13(a)–(h) show the images where all components are changed.

DISCUSSION

From Fig. 10(a)–(h) to Fig. 12(a)–(h), we can recognize age-related changes such as pigmented spots, redness of cheeks, and shape-included shading. These images show that the melanin components and the shading components especially have a relationship with age-related changes. In the melanin component changes shown in Fig. 10(a)–(h), the increase of pigmentation unevenness on cheeks and the pigmentation distribution around the eyes are represented by modulating the first and second principal components shown in Fig. 9(a). In the hemoglobin component changes shown in

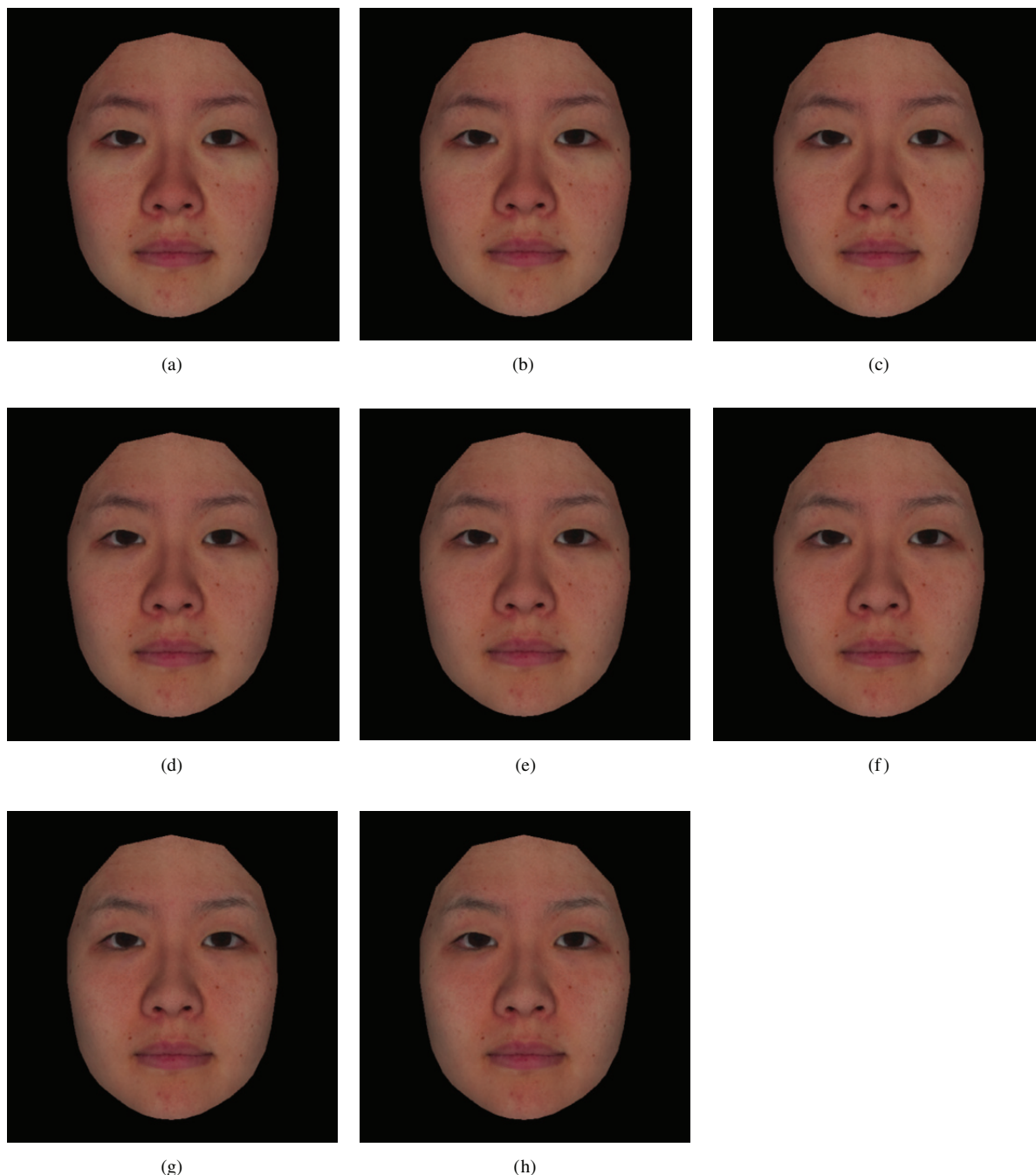


Figure 11. Results of facial appearance by age-related changes in hemoglobin components: (a) 10s, (b) 20s, (c) 30s, (d) 40s, (e) 50s, (f) 60s, (g) 70s, (h) 80s.

Fig. 11(a)–(h), the age-related changes are simulated mainly by the decrease of the first principal component and the increase of the second principal component in Fig. 9(b). In the shading component changes shown in Fig. 12(a)–(h), the age-related changes are simulated mainly by modulation of the first principal component in Fig. 9(c). These changes are observed as shape-related changes, such as hollows around the eyes and sagging of the jaw.

In addition, we performed a subjective evaluation of the reproduced images. The evaluator was a face expert who worked in the beauty industry. The results of the subjective

Table I. Results of an expert’s subjective evaluation of the reproduced images.

Reproduced age	Estimated age
20	26.8
40	27.3
60	30.5
80	35.3

evaluation are shown in Table I. The results show that the modulation of pigmentation distribution is appropriate

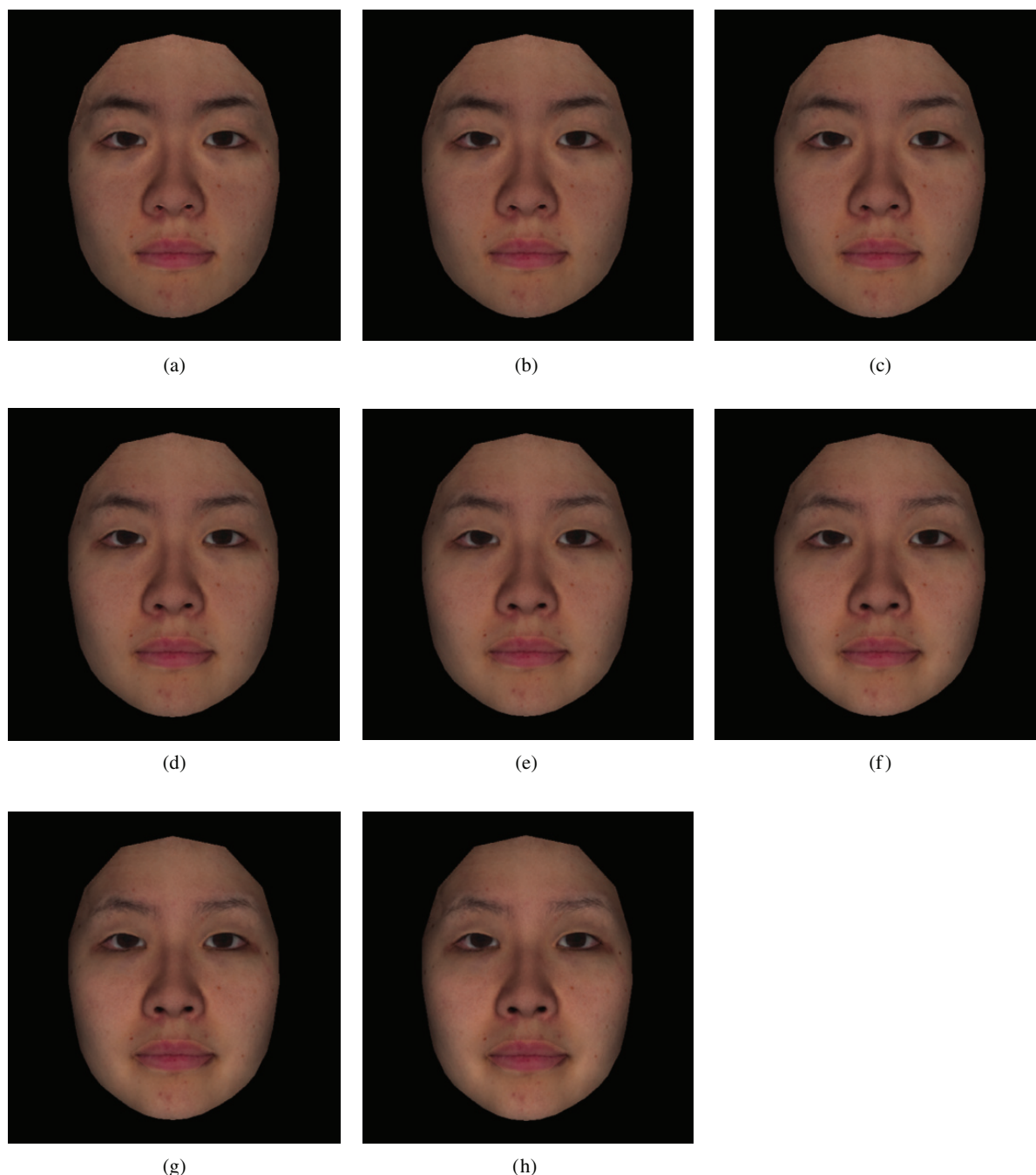


Figure 12. Results of facial appearance by age-related changes in shading components: (a) 10s, (b) 20s, (c) 30s, (d) 40s, (e) 50s, (f) 60s, (g) 70s, (h) 80s.

for age-related changes from the perspective of physiology. However, the age in Fig. 13(h) estimated by the expert was 35.3 years old instead of the reproduced age which was in the eighties. The reproduced images looked younger than the reproduced age in many instances. We considered that this occurred because we did not modulate the facial structures and detailed surfaces such as wrinkles. Lantis et al.⁵ did not consider pigmentation distribution and shading, but they obtained good results in modulating the facial structure. Facial structure is a critical factor for the appearance of a face and needs to be taken into account in future work.

CONCLUSION

In this article, we extracted melanin and hemoglobin pigmentations from a single skin color image by independent component analysis. First, normalized facial images were obtained by morphing the shapes of facial images to that of an average face. Next, we applied PCA to pigmentation distributions in a whole face and obtained the feature values of uneven pigmentation. Then, we estimated the relationship between the obtained feature values and age by multiple regression analysis. After the weights of the principal components were modulated based on the estimated

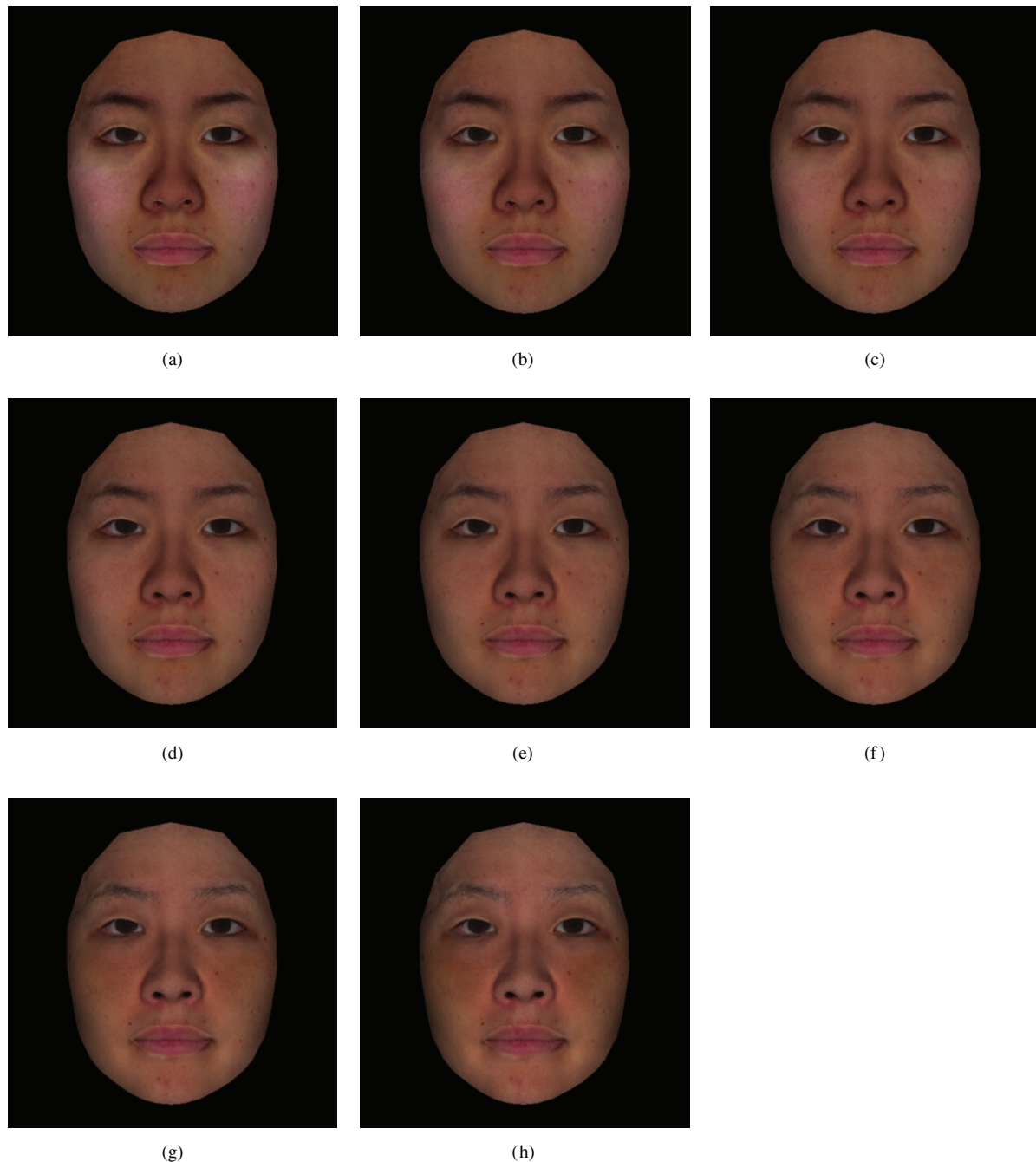


Figure 13. Results of appearance of face by age-related changes in all components: (a) 10s, (b) 20s, (c) 30s, (d) 40s, (e) 50s, (f) 60s, (g) 70s, (h) 80s.

relationship, the appearance of a face was simulated by age-related changes.

In future work, we will analyze the feature values of the facial structure and the detailed surface, and more realistically simulate the appearance of a face having arbitrary physiological features. We also need to explore the generality of the feature values. In addition, the approximately 30 min of computing time and the need for some manual operations are problems. It will not be practical to use our application until we have speeded up and automated the processes.

ACKNOWLEDGMENTS

This research was partly supported by JSPS Grants-in-Aid for Scientific Research (24560040).

REFERENCES

- ¹ T. Makino, N. Tsumura, K. Takase, R. Homma, T. Nakaguchi, N. Ojima, and Y. Miyake, "Development of the measurement system for facial physical properties with the short-distance lighting," *J. Imaging Sci. Technol.* **53**, 060501-1-060501-9 (2009).
- ² T. Makino, K. Takase, K. Ochiai, N. Tsumura, T. Nakaguchi, and N. Ojima, "Computational lighting reproduction for facial live video

- with rigid facial motion," *J. Imaging Sci. Technol.* **55**, 010503-1–010503-7 (2011).
- ³ K. Scherbaum, T. Ritschel, M. Hullin, T. Thormählen, V. Blanz, and H.-P. Seidel, "Computer-suggested facial makeup," *Comput. Graph. Forum* **30**, no. 2, 485–492 (2011).
 - ⁴ D. Guo and T. Sim, "Digital face makeup by example," *Comput. Vis. Pattern Recognit.* 73–79 (2009).
 - ⁵ A. Lantis, C. J. Taylor, and T. F. Cootes, "Toward automatic simulation of aging effects on face images," *IEEE Trans. Pattern Anal. Mach. Intell.* **24**, no. 4, 442–455 (2002).
 - ⁶ C. Liewchavalit, M. Akiba, T. Kanno, and T. Nagao, "Extracted facial feature of racial closely related faces," *Proc. SPIE* **7546**, 75461R (2010).
 - ⁷ N. Tsumura, H. Haneishi, and Y. Miyake, "Independent component analysis of skin color image," *J. Opt. Soc. Am.* **16**, no. 9, 2169–2176 (1999).
 - ⁸ N. Tsumura, N. Ojima, K. Sato, M. Shiraishi, H. Shimizu, H. Nabeshima, S. Akazaki, K. Hori, and Y. Miyake, "Image-based skin color and texture analysis/synthesis by extracting hemoglobin and melanin information in the skin," *ACM Trans. Graph. (TOG)* **22**, 770–779 (2003).
 - ⁹ N. Tsumura, T. Nakaguchi, N. Ojima, K. Takase, S. Okaguchi, K. Hori, and Y. Miyake, "Image-based control of skin melanin texture," *Appl. Opt.* **45**, no. 25, 6626–6633 (2006).
 - ¹⁰ S. S. Mukaida, M. G. Kamachi, M. Oda, T. Kato, S. Yoshikawa, S. Akamatsu, and K. Chihara, "Facial image synthesis system: futon-evaluation as tools for cognitive research on face processing," *IEICE Trans. Fundam.* **J85A**, no. 10, 1126–1137 (2002) (in Japanese).
 - ¹¹ M. Hiraoka, M. Firbank, M. Essenpreis, M. Cope, S. R. Arridge, P. van der Zee, and D. T. Delpy, "A Monte Carlo investigation of optical path length in inhomogeneous tissue and its application to near-infrared spectroscopy," *Phys. Med. Biol.* **38**, 1859–1876 (1993).
 - ¹² M. S. Drew, C. Chen, S. D. Hordley, and G. D. Finlayson, "Sensor transforms for invariant image enhancement," *Proc. IS&T/SID Tenth Color Imaging Conf.* (IS&T, Springfield, VA, 2002), pp. 325–330.
 - ¹³ D. Pissarenko, "Neural Networks for Financial Time Series Prediction: Overview over Recent Research," B.Sc. thesis (2002).